

Structure dependence of Compton profiles. Model study*

B. Kramer[†] and P. Krusius[‡]

Institut für Physik, Universität Dortmund, 4600 Dortmund 50, Federal Republic of Germany

(Received 23 May 1977)

In order to test the usefulness of Compton scattering for the investigation of structural effects on the ground state of solids, the structure dependence of the density of states (DOS), momentum density (MD), and Compton profile (CP) has been studied using various ordered and disordered arrays of atom potentials of the Koster-Slater impurity type. For the crystalline arrays the results are exact within the one-electron approximation. The dependence of the crystalline DOS, MD, and CP on the atom density and the anisotropy of the structure is discussed. For the disordered distribution of atoms the results are exact within the coherent-potential approximation. The results show that disorder is seen as a more atomiclike behavior of the MD and the CP, and that the disorder-induced changes in these quantities are detectable with the presently achievable experimental accuracy. In addition, approximate methods for evaluating MD's and CP's are discussed and conclusions on their quality drawn.

I. INTRODUCTION

The differential scattering cross section for Compton scattering is according to the impulse approximation^{1,2} directly related to the ground state of the electron system considered. Therefore, in principle, Compton scattering is an ideal tool for studying structural properties of various phases of solids. The present state of the art in experimental Compton spectroscopy may be characterized by two numbers (γ -ray case): total momentum resolution 0.4 a.u. and statistical counting accuracy 0.5%.³ In addition to these uncertainties, aspects such as multiple scattering, separation of the background, relativistic effects, and core corrections have to be considered at least for systems with heavier constituents. Since structural properties influence, to a first approximation, only the valence contribution to the scattering process, it is not clear at present to which extent different phases of a given material are distinguishable in the experiment.

Theoretical calculations of Compton profiles (CP) are based on the impulse approximation,² which relates the CP and the ground-state momentum density (MD) to each other. The calculation of MD's is, however, a difficult problem even in the one-electron approximation. Methods, such as the linear combination of atomic orbitals^{4,5} (LCAO) or the pseudopotential approach^{6,7} used extensively to determine primarily energy-dependent properties of periodic solids, are only valid for restricted energy ranges, and may lead to systematic errors, the magnitude of which is hard to estimate. Even in the case of density-functional based self-consistent methods, such as self-consistent orthogonalized plane wave⁸ (SCSOPW) or self-consistent discrete variational method⁹ (SCDVM), correlation effects are at best incorporated in a statistical fashion.

Again there are no quantitative estimates of these effects on the ground-state properties of periodic solids. For solids without long-range order or for large molecules, there are not even methods for treating the electronic ground state at a comparable level within the one-electron approximation. In particular, for solids with only a well-defined short-range order a theoretical description of the ground state is still unavailable.

Thus, a number of basic questions on the ground-state properties of periodic and nonperiodic solids require answers to which Compton spectroscopy is likely to be able to contribute, since it sensitively only depends on the electronic ground state contrary to, e.g., optical spectra which involve excited states of the system. The ground state, on the other hand, is determined both by the constituent atoms and by their structural arrangement. This has been shown to be true long ago for the momentum distribution of simple molecular systems in the pioneering work of Coulson *et al.*¹⁰ Also, for a specific ionic crystal, the CP has been demonstrated to be orders of magnitudes more sensitive to anisotropy than x-ray form factors.⁵ Therefore, CP's should, in general, be sensitive to changes in the local arrangement of the atoms in the different phases of a given material. Of special interest in this context are the disordered phases, e.g., the amorphous semiconductors, for which first studies have revealed large differences in the CP with respect to their crystalline counterparts.¹¹

The aim of the present work is to study these structural effects quantitatively, in order to explore their influence on the CP and in order to see whether these effects are measurable with the present experimental technique. The electronic density of states (DOS) and the ground-state MD and CP are the key quantities considered in this model study resulting in answers exact in a sense defined

below. In Sec. II, the model solids are defined. The results for the Green's functions for these systems are derived in Appendices A, B, and C. The ground-state properties DOS, MD, and CP are presented in Sec. III. Approximations for the momentum density are considered in Sec. IV. In the discussion in Sec. V crystal formation, structural changes between crystalline phases, and order-disorder transitions are considered in order to obtain information on the sensitivity of the CP. In Sec. V, the LCAO approximation for the MD is also discussed in comparison with the exact results. This provides criteria for the validity of approximate methods when evaluating ground-state properties of real solids.

II. MODEL

Consider a solid of volume Ω consisting of N model potentials each of which may be assigned only one s -like valence state. Such model atoms can be represented by the scattering operator (in free-electron representation)^{12,13}

$$t(\vec{k}, \vec{k}', E) = 4\pi/(K_0 + i\sqrt{E}) = t(E). \quad (1)$$

$t(E)$ has a pole at the energy $E_0 = -K_0^2$ of the s -like state and corresponds to the potential

$$v(\vec{k}, \vec{k}') = \begin{cases} -4\pi/v_0, & |\vec{k} - \vec{k}'| \leq \pi k_0 \\ 0, & \text{otherwise} \end{cases} \quad (2)$$

in the limit $v_0 \rightarrow \infty$, $k_0 \rightarrow \infty$ with $K_0 = 2k_0 - v_0$ remaining finite (Appendix A).

The specific structures studied are (i) the crystal lattice with one atom per unit cell and (ii) the random distribution of atoms. For the crystal, the one-electron Green's function can be determined exactly and for the random distribution it can be evaluated exactly within the coherent-potential approximation^{14,15} (CPA). Using the one-electron self-energy $S(\vec{k}, E)$, one obtains for the diagonal part of the Green's function

$$G(\vec{k}, E) = 1/[E - k^2 - S(\vec{k}, E)]. \quad (3)$$

The expressions for $S(\vec{k}, E)$ for the crystal and for the random case are given in the Appendices B and C, respectively.

III. GROUND-STATE PROPERTIES AND COMPTON PROFILE

In the impulse approximation the CP, $J_{\vec{k}}(q)$, is related to the MD of the ground state $N(\vec{p})$:

$$J_{\vec{k}}(q) = \frac{1}{(2\pi)^3} \int d^3p N(\vec{p}) \delta(\omega - k^2 - 2\vec{k} \cdot \vec{p}), \quad (4)$$

where $q = (\omega - k^2)/2k$, and ω and \vec{k} denote the energy and momentum transfer, respectively. In the one-electron approximation, the MD is given by ($T=0$ K)

$$N(\vec{p}) = \frac{1}{N} \sum_j^{\text{occ}} |\psi_j(\vec{p})|^2, \quad (5)$$

$$\frac{1}{(2\pi)^3} \int d^3p N(\vec{p}) = 1,$$

where the $\psi_j(\vec{p})$'s are Fourier transformed one-electron wave functions. The sum includes all occupied states j . $N(\vec{p})$ is related to the one-electron Green's function via

$$N(\vec{p}) = -\frac{1}{N} \frac{1}{\pi} \text{Im} \int_{-\infty}^{E_F} dEG(\vec{p}, E^*). \quad (6)$$

The density of states is given by

$$n(E) = -\frac{1}{\pi} \frac{1}{N} \int d^3p \text{Im} G(\vec{p}, E^*), \quad (7)$$

and the Fermi energy E_f by

$$\int_{-\infty}^{E_F} n(E) dE = 1. \quad (8)$$

In general the ground-state MD is related to the one-electron density matrix $\gamma_1(\vec{r}, \vec{r}')$ via the Fourier transformation

$$N(\vec{p}) = \int d^3r \int d^3r' e^{-i\vec{p} \cdot (\vec{r} - \vec{r}')} \gamma_1(\vec{r}, \vec{r}'). \quad (9)$$

Thus, $N(\vec{p})$ and consequently also $J_{\vec{k}}(q)$ contain information on the nondiagonal parts of the first-order density matrix $\gamma_1(\vec{r}, \vec{r}')$. This is complementary to elastic x-ray scattering, which only provides information on the diagonal part of $\gamma_1(\vec{r}, \vec{r}')$.

Using the Green's functions of the model systems described in Sec. II, it is straightforward to determine $n(E)$ and $N(\vec{p})$. For the random distribution, as well as for the isolated atom, the MD is isotropic and the CP reduces to the one-dimensional integral

$$J(q) = \frac{1}{(2\pi)^2} \int_{|q|}^{\infty} dp p N(|\vec{p}|). \quad (10)$$

For the crystal, $N(\vec{p})$ also depends on the direction of \vec{p} , and the two-dimensional integrals associated with the CP have been evaluated numerically.⁸

Results for $n(E)$, $N(\vec{p})$, and $J(q)$ are shown in Figs. 1 and 2 for two densities of atoms δ defined as $\delta = 4\pi N/(\Omega K_0^3) \cdot \delta = 1$ corresponds to an ordinary density with sizeable nearest-neighbor interactions. Two different crystal structures, the simple cubic crystal and the simple tetragonal crystal with the lattice constant ratio $\gamma = c/a = 2$, have been considered. A relative convergence threshold of 0.001 for the MD was used in all cases. In Fig. 3, the anisotropy of the Compton profile (ACP), defined as

$$\Delta J_{\vec{k}-\vec{k}'}(q) = J_{\vec{k}}(q) - J_{\vec{k}'}(q), \quad (11)$$

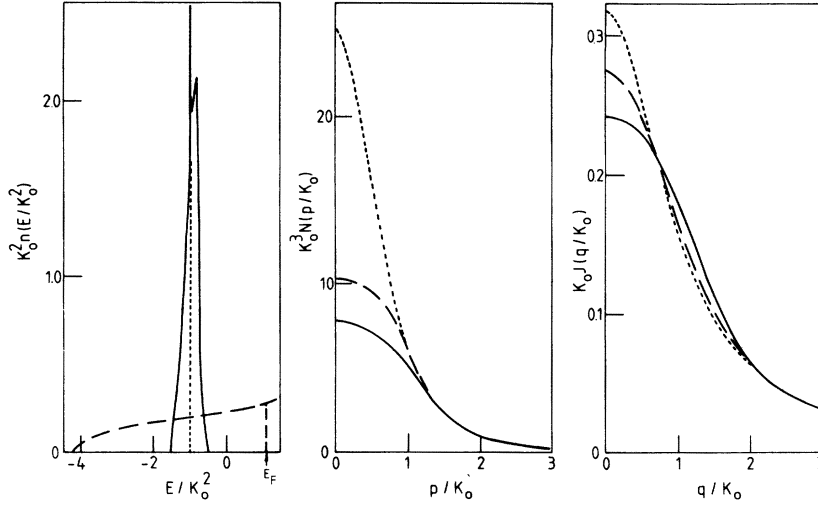


FIG. 1. Density of states, momentum density, and Compton profile for two model solids with the density of atoms $\delta = 1$. Simple cubic crystal (full curve) and random distribution (broken curve). For the simple cubic structure, the momentum density and Compton profile are shown along the [100] bonding direction. For reference, the results for the isolated atom have also been plotted (dotted curve). All quantities are shown in reduced units (see Appendix A).

has been plotted for $\delta = 1$, and $\gamma = 1$ and 2 for characteristic directions. Figures 4 and 5 display contour maps of $N(\vec{p})$ for $\delta = 1$ and $\gamma = 1$ and 2, respectively. Finally, in Fig. 6, the difference CP's (DCP) between the isolated atom and the random and crystalline phases are shown for $\delta = 1$, and $\gamma = 1$ and 2.

IV. APPROXIMATIONS FOR THE MOMENTUM DENSITY

A rigorous first-principles evaluation of the ground-state MD of a real material is very complicated or even impossible at present, as, for example, for the amorphous phase of semiconductors. It is thus imperative to search for realistic approximations involving as few adjustable parameters as possible. For wave-function dependent ground-state properties, such as the MD, the LCAO method might be a suitable approach, which

could include orthogonalization effects with respect to the core and also, to some extent, self-consistency effects. For the present model systems, with only one s -like state per atom, the LCAO scheme turns out to be particularly simple.

The LCAO Bloch function for the description of a periodic solid is in the present case

$$\psi_{\vec{k}}(\vec{r}) = a_{\vec{k}} \sum_{\vec{R}_1} e^{i\vec{k} \cdot \vec{R}_1} \phi(\vec{r} - \vec{R}_1), \quad (12)$$

where $\phi(\vec{r})$ denotes an s -like normalized atomic function. $a_{\vec{k}}$ is the normalization constant. $a_{\vec{k}}$ clearly depends on the overlap between the atomic functions and is only for orthogonal ϕ 's a constant equal to $(N)^{-1/2}$. $a_{\vec{k}}$ may be written as

$$|a_{\vec{k}}|^2 = \frac{1}{N} \left[\sum_{\vec{m}} |\phi(\vec{k} - \vec{G}_m)|^2 \right]^{-1}. \quad (13)$$

Here \vec{G}_m is a reciprocal-lattice vector and $\phi(\vec{r})$ the

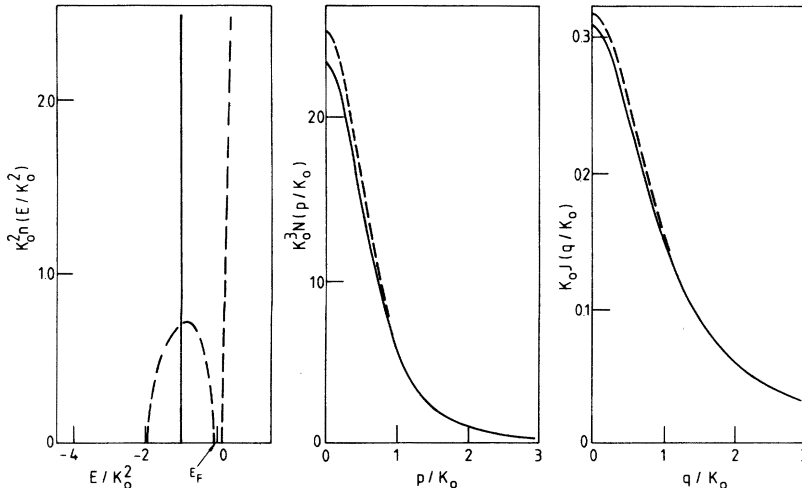


FIG. 2. Density of states, momentum density, and Compton profile as in Fig. 1, but for the density of atoms $\delta = 0.1$.

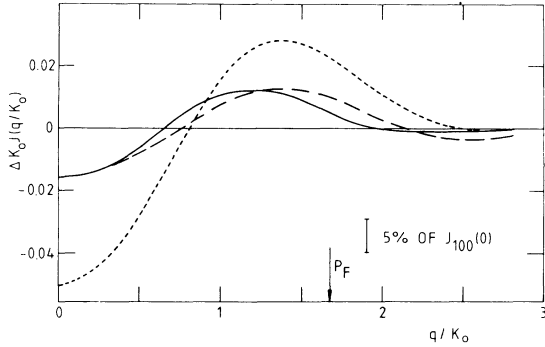


FIG. 3. Anisotropy of the Compton profile for the simple cubic (sc) and simple tetragonal (st) phases with the density of atoms $\delta=1$. sc [100]-[110] directions (full curve), st [100]-[110] directions (broken curve), and st [100]-[001] directions (dotted curve). p_F denotes the Fermi momentum.

Fourier transform of $\phi(\vec{r})$. For a crystal with one atom in the unit cell and one state per atom, one obtains (Eq. 5)

$$N(\vec{p}) = \frac{1}{N} \left[\sum_{\vec{m}} |\phi(\vec{p} - \vec{G}_m)|^2 \right]^{-1} |\phi(\vec{p})|^2. \quad (14)$$

For the random distribution of atoms a more complicated parametrization has to be made. For

$$A(\vec{R}_1 - \vec{R}_2) = \int_{\vec{R}_3, \dots, \vec{R}_N} \prod_{i=3}^N d^3R_i P(\vec{R}_1, \vec{R}_2 | \vec{R}_3, \dots, \vec{R}_N) \int_{-\infty}^{E_F} dE G_{12}(E; \vec{R}_1, \dots, \vec{R}_N). \quad (19)$$

In Eq. (18), the factorization¹⁶

$$P(\vec{R}_1, \dots, \vec{R}_N) = P_1(\vec{R}_1) P_2(\vec{R}_1 | \vec{R}_2) \times P(\vec{R}_1, \vec{R}_2 | \vec{R}_3, \dots, \vec{R}_N) \quad (20)$$

has been used. $P(\vec{R}_1, \vec{R}_2 | \vec{R}_3, \dots, \vec{R}_N)$ denotes the conditional probability of finding atoms at $\vec{R}_3, \dots, \vec{R}_N$ once two atoms are fixed at \vec{R}_1 and \vec{R}_2 . For a disordered system, macroscopic homogeneity and isotropy imply that

$$P_1(\vec{R}_1) = \Omega^{-1}, \quad P_2(\vec{R}_1 | \vec{R}_2) = P_2(|\vec{R}_1 - \vec{R}_2|). \quad (21)$$

Thus $\langle f(\vec{p}) \rangle$ (Eq. 18) has been decomposed into a purely structural part P_2 and a second part depending on the interactions between atoms. In the case of a periodic configuration $f(\vec{p})$ is given by the prefactor of $|\phi(\vec{p})|^2$ in Eq. (14) and is a periodic function in \vec{p} space. Further, for a completely random distribution of atoms, in addition to P_1 , also $P_2(|\vec{R}_1 - \vec{R}_2|) = \text{const.}$ and hence $\langle f(\vec{p}) \rangle$ is simply the Fourier transform of $A(\vec{x})$.

In order to investigate the quality of the LCAO approximations (14) and (16) a choice of the atomic function ϕ has to be made. The simplest possibility is to use that of the isolated atom (Appendix

a configuration $\vec{R}_1, \dots, \vec{R}_N$, the LCAO ansatz

$$\psi_j(\vec{r}) = \sum_i c_{ji}(\vec{R}_1, \dots, \vec{R}_N) \phi(\vec{r} - \vec{R}_i) \quad (15)$$

results formally in

$$N(\vec{p}) = f(\vec{p}) |\phi(\vec{p})|^2, \quad (16)$$

where $\phi(\vec{p})$ only depends on the atomic part and $f(\vec{p})$ contains the details of the structure associated with the particular configuration. In terms of the Green's function one may write

$$f(\vec{p}) = \frac{1}{N} \frac{1}{\pi} \text{Im} \sum_{i,j} e^{i\vec{p} \cdot (\vec{R}_i - \vec{R}_j)} \int_{-\infty}^{E_F} dE G_{ij}(E) \quad (17)$$

with $G_{ij}(E) = \langle \phi_i | G(E) | \phi_j \rangle$. The structural factor $f(\vec{p})$ depends both on the atomic positions $\vec{R}_1, \dots, \vec{R}_N$ and the interatomic interaction represented by $G_{ij}(E)$, the probability amplitude for an electron with the energy E going from the state $\phi(\vec{r} - \vec{R}_i)$ into the state $\phi(\vec{r} - \vec{R}_j)$. Taking the average overall configurations $\{\vec{R}_1, \dots, \vec{R}_N\}$ by using the associated normalized probability density $P(\vec{R}_1, \dots, \vec{R}_N)$ one obtains

$$\langle f(\vec{p}) \rangle = 1 - \text{Im} \int d^3x e^{i\vec{p} \cdot \vec{x}} P_2(\vec{x}) A(\vec{x}), \quad (18)$$

where

A) such that the binding energy is left as an adjustable parameter K to account for the interatomic interactions in the solid, i.e.,

$$|\phi(\vec{p})|^2 = 8\pi K / (K^2 + p^2)^2. \quad (22)$$

By comparing the exact MD's (Appendices B and C) with the LCAO counterparts one obtains $f(\vec{p})$ as a function of the parameter K . If it would be possible to find a good fit for some value K such that $f(\vec{p}) = \text{const.}$, all interatomic interactions had been included into the atomic function. Such a solution is, however, in general not possible and would in the present case mean that, e.g., all crystalline anisotropy effects would vanish.

Consider first the LCAO results for the crystalline case. In Figs. 7 and 8 the best fit of Eq. (14) to the exact result for the MD (Appendix B) is shown for $\delta=1, \gamma=1$ and $\delta=1, \gamma=2$, respectively. The corresponding LCAO CP's have not been evaluated, since the latter differences are even smaller, a statement which may be verified, e.g., by studying the examples given in Figs. 1 and 2. For the random array of atoms with $\delta=1$ the ratio $N(\vec{p})_{\text{exact}} / |\phi(\vec{p})|^2 = f'(\vec{p})$ has been plotted in Fig. 9.

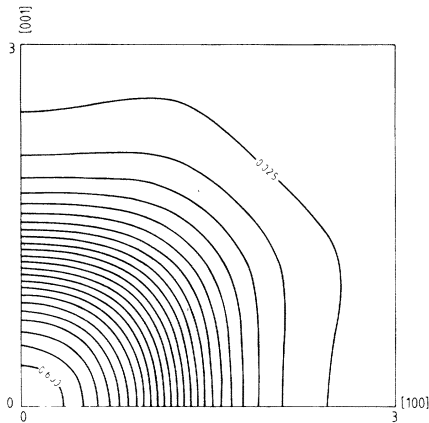


FIG. 4. Contour map of the simple cubic crystalline momentum density. The density of atoms is $\delta=1$. The contour plane includes the origin of the momentum space and the directions [100] and [001]. The width of the contour plane is 3, and the contour increment $4\pi \times 0.025$ reduced atomic units.

For comparison, Fig. 9 also shows the corresponding $f'(\vec{p})$ for the crystal with $\delta=1$ and $\gamma=1$.

V. DISCUSSION

Consider first, the question concerning the sensitivity of the CP with respect to changes in the MD. By comparing the results shown in Figs. 1 and 2, one realizes that the two-dimensional integral smoothens most of the rather large differences in the MD's. For example, the ratio of the atomic and crystalline MD's is maximally 3.2 for the density $\delta=1$, whereas the corresponding ratio for the CP's is only about 1.3. Numbers like these of course strictly apply only to the present model systems, but quantitatively similar effects are also true for more complicated systems.⁸

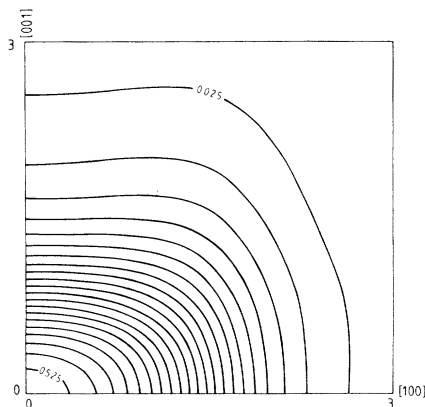


FIG. 5. Contour map of the simple tetragonal crystalline momentum density. For additional information see caption of Fig. 4.

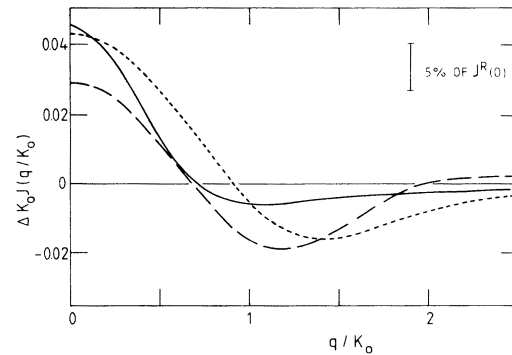


FIG. 6. Difference Compton profile between the isolated atom (IA), the random array (R), and the simple cubic (sc) and simple tetragonal (st) crystals. IA-R (full curve), R-sc [100] (broken curve), and R-st [100] (dashed curve where applicable $\delta=1$ has been used).

A physically more interesting aspect is the sensitivity of the CP against structural changes in the system. Figure 3 shows that the CP exhibits a significant anisotropy even for the simple cubic lattice. For an energy transfer of the order of the Fermi momentum p_F , the CP along the nearest-neighbor bond direction [100] is higher than in the nonbonding direction [110]. For small q the effect is reversed because of vanishing anisotropy for large q and because of norm conservation. This behavior of the CP reflects the well-known empirical rule on the MD, namely that bond formation enhances the

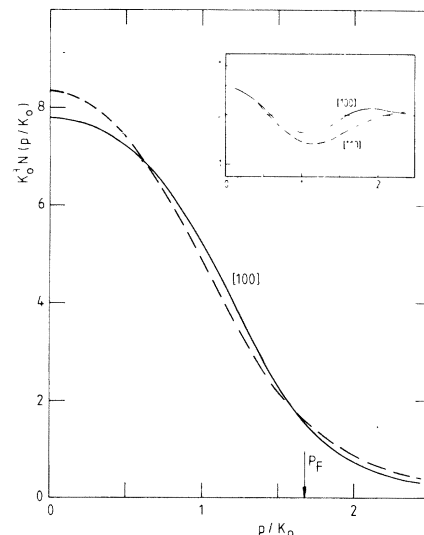


FIG. 7. Momentum density of the simple cubic crystal with $\delta=1$ in the [100] direction. Exact result (full curve) and optimal fit of LCAO model with $K=1.22$ (broken curve). Inset shows the difference between the LCAO and the exact results in the [100] (full curve) and in the [110] (broken curve) directions also in reduced units. p_F denotes the Fermi momentum.

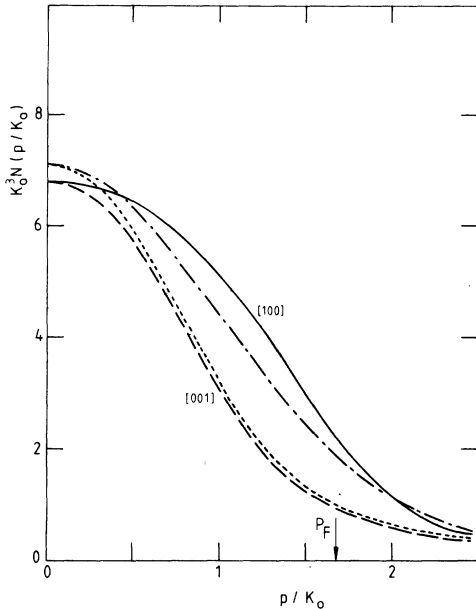


FIG. 8. Momentum density of the simple tetragonal crystal with $\delta=1$ in the [100] and [001] directions. [100], exact result (full curve); [001], exact result (broken curve); [100] LCAO fit with $K=1.30$ (chain curve); and [001] LCAO fit with $K=1.30$ (dotted curve). p_F denotes the Fermi momentum.

higher-momentum components perpendicular to the bonds at the cost of the parallel ones. The contour maps for the simple cubic and simple tetragonal lattices in Figs. 4 and 5 prove that this rule also applies to the present s -like systems. Quantitatively the largest changes in the MD's associated with crystal formation are not seen at momenta involved in bond formation, but as a result of norm conservation in a region close to the origin of the momentum space. Furthermore, from Fig. 3 one realizes that there may be anisotropies of the CP, which are quite insensitive to major changes in the

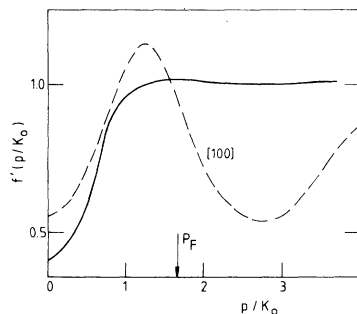


FIG. 9. Ratio of exact momentum density and effective atomic momentum density for $\delta=1$. Random case with LCAO parameter $K=1.01$ (full curve), and simple cubic crystal with LCAO parameter $K=1.22$ (broken curve).

system. For example, the doubling of the lattice constant in the [001] direction introduces only small changes into the anisotropies perpendicular to this direction. This behavior parallels the experimental findings for the group-IVA semiconductors C, Si, and Ge.¹⁷ The ACP's of these materials, when scaled to equal density, are almost the same for nonbonding directions ([110]–[100]), whereas ACP's involving the bonding directions (e.g., [111]–[100]) differ. One may thus conclude that ACP's between nonbonding directions are mainly an effect of the geometrical structure, while CP differences associated with bonding directions are more sensitive to changes in the chemical bond itself. A strict separation is of course not possible, since the structure is determined by the chemical bond and vice versa.

In a structural change relaxing the long-range order of the crystalline phase, more drastic effects are seen (Figs. 1, 2, and 6). The MD and CP of the disordered system show a more atomiclike behavior, i.e., the widths of both the MD and CP are smaller and consequently the values $N(0)$ and $J(0)$ are larger than in the crystal. This means for the disordered ground state a decrease of the probability density associated with intermediate-momentum components, when compared with the crystal. One may thus deduce that the expectation value of the kinetic energy of the electrons, or via the virial theorem, the cohesive energy, for the disordered system should be smaller than for the crystal. In addition, in the low-density case (Fig. 2), the MD for the random distribution of atoms turns out to equal almost quantitatively that of an isolated atom, whereas the DOS is still considerably broadened by the interatomic interactions. Although the CPA, together with the assumption of the completely random distribution involving large overlap matrix elements, seems to overestimate these trends, the conclusion is that disorder in general broadens the DOS,¹⁸ and just the opposite is true for the MD and the CP. Considering the differences between the CP's of the isolated atom and the random array and, on the other hand, of the latter and the crystalline lattices shown in Fig. 6, one realizes that qualitatively all differences are similar. The CP of the random array thus seems to interpolate between the CP's of the isolated atom and the crystal lattice. If one extends this result to real amorphous materials, it means that different amorphous phases may have a more atomiclike or more crystalline CP depending on the involved degree of the short-range order.

The effects of structural changes on the CP discussed above have been experimentally verified for the anisotropic semiconductor Se.^{19,11} For example, the experimental $J(0)$ value of the studied am-

orphous phase is about 5% larger than that of the polycrystalline trigonal phase. Also the difference of the CP's between the amorphous and polycrystalline phases as a function of q behaves qualitatively similar as in the present case.

Consider finally the approximate LCAO methods discussed in Sec. IV. The crystalline results for a realistic density of atoms ($\delta = 1$) in Figs. 7 and 8 show that, with a suitable choice of the atomic function, the simple LCAO fit describes qualitatively correctly both the absolute values and the anisotropy. Effects of self-consistency are of importance for nearest-neighbor [100] bonding directions and also for the nonbonding directions, such as the [110] direction shown in the inset of Fig. 7; however, considering that there is only one parameter involved the fit is good. Therefore, even for ordinary densities of atoms, the LCAO approach seems to work reasonably for wave-function dependent properties of the electronic ground state, such as the MD and the CP. Of course, LCAO results may also be used together with experimental CP's in order to deduce the realistic form of the effective atomic functions and of the interatomic interactions, but usually there is more than one state per atom and then the situation is more complicated.

As an extension of the above statements, concerning the quality of wave-function dependent LCAO results, some more general remarks may be made. If one uses the LCAO approximation in order to calculate MD's and CP's, care must be exercised to include, in addition to the correct matrix elements of the Hamiltonian and the overlap matrix elements, wave functions of the correct shape, as has been done, e.g., in the case of the simple ionic crystal LiF.⁵ However, although such a procedure guarantees realistic MD's and CP's, it does not need to result in correct anisotropies or difference profiles between different phases of more complicated systems. A second point is that convergence criteria depending exclusively on energy spectra are completely insufficient. For example, for the simple cubic crystalline phase with $\delta = 0.1$, a relative convergence threshold of 0.001 for the poles of the exact one-particle Green's function lead to stochastic steps in the MD, which were roughly by a factor of 1000 larger than those in the energy bands. A systematic investigation of the convergence of wave-function dependent properties in the LCAO approach is, however, in practice impossible.

From the LCAO results one may also learn that to a good approximation the interactions between the excited and occupied states may be neglected when considering ground-state properties of solids. It should be noted that this conclusion is based on

wave-function dependent ground-state properties and not on energy spectra. From this, the associated well-known statement for the ground-state energy spectra, namely, that the LCAO approach provides a good description of valence-band energy spectra, follows directly. On the other hand, the LCAO results also show that the interatomic interactions of occupied states are important for ground-state properties, since $f'(\vec{p})$ deviates from a constant for all model systems considered. In particular, one realizes that for the disordered array $f'(\vec{p})$ remains essentially constant for momenta above $p \approx 2\pi/a$, where a is the mean atomic separation. This indicates that the interatomic interactions described by $A(\vec{x})$ (Eq. 18) are large only for distances $x \lesssim a$. For the crystal $f'(\vec{p})$ is not strictly a periodic function of \vec{p} as it is in the present LCAO approximation. The decomposition of the MD in the LCAO approximation into a purely structure-dependent part and an atomic part is interesting from another point too. Equations (16), (18), and (19) provide the first step for investigating the structure dependence of the CP for more complicated systems with more than one atom per unit cell and, what is more important, with short-range order.

VI. CONCLUSIONS

A number of new conclusions may be drawn from the present work constituting the first systematic contribution to the structure dependence of the Compton profile of ordered and disordered solids. The most importance of these are the following. First, the anisotropy of the CP of the crystalline phases appears to react most sensitively to changes in the geometrical structure, or, in the chemical bonding, only in those directions for which these changes take place. This behavior suggests a quantitative explanation of the experimental data on C, Si, and Ge. Second, contrary to the DOS, the widths of the MD and the CP decrease from the crystalline phase to the random array of atoms. This conclusion is confirmed by experimental data on Se. Third, although the LCAO approximation results in qualitatively correct CP's, it does not always guarantee correct anisotropies until effects of self-consistency and convergence are properly included.

VII. ACKNOWLEDGMENTS

The authors wish to express their gratitude towards Professor J. Treusch for critical comments during the preparation of the manuscript. Stimulating discussions with members of the experimental section of the Compton group at the University of Dort-

mund, Professor U. Bonse, Dr. W. Schülke, and Dr. W. Schröder, are gratefully acknowledged.

APPENDIX A: ISOLATED ATOM

The atom potential is defined in the plane-wave basis by

$$v(\vec{k}, \vec{k}') = \begin{cases} -4\pi/v_0, & |\vec{k} - \vec{k}'| \leq k_0 \\ 0 & \text{otherwise.} \end{cases} \quad (\text{A1})$$

The scattering matrix fulfills the integral equation

$$t(\vec{k}, \vec{k}', z) = v(\vec{k}, \vec{k}') + \sum_{\vec{k}''} v(\vec{k}, \vec{k}'') \times \frac{1}{z - \vec{k}''^2} t(\vec{k}'', \vec{k}', z), \quad (\text{A2})$$

where z is a complex energy variable. Combining (A1) and (A2) one obtains for $|z| \ll (\pi k_0)^2$ a $t(\vec{k}, \vec{k}', z)$, which is independent of \vec{k} and \vec{k}' . For real $z = E$

$$t(E) = -\frac{4\pi}{v_0 + 4\pi F(E)},$$

$$F(E) = \lim_{\eta \rightarrow 0} \sum_{\vec{k}, |\vec{k}-\vec{k}''| \leq \pi k_0} \frac{1}{E + i\eta - k''^2}$$

$$= -\frac{i}{4\pi} \sqrt{E} - \frac{1}{2\pi} k_0. \quad (\text{A3})$$

Since $t(E)$ has a pole at $E = -K_0^2$ with $K_0 = 2k_0 - v_0$, there is a bound state for v with this energy. The Green's function is diagonal in the momentum \vec{p}

$$G(\vec{p}, E) = G_0(\vec{p}, E) + G_0^2(\vec{p}, E) 4\pi/K_0 + i\sqrt{E},$$

$$G_0(\vec{p}, E) = 1/(E - p^2). \quad (\text{A4})$$

The associated MD in a volume Ω normalized ac-

$$S(\vec{k}, \vec{k}', z) = d \left(-\frac{4\pi}{v_0} \right) \sum_{m \neq 0; |\vec{G}_m| \leq \pi k_0} \left[\delta_{\vec{k}-\vec{k}', \vec{G}_m} + \frac{1}{z - |\vec{k} - \vec{G}_m|^2} S(\vec{k} - \vec{G}_m, \vec{k}', z) \right]. \quad (\text{B4})$$

Here $d = N/\Omega$ denotes the density of atoms. Iteration yields for the diagonal part of S

$$S(\vec{k}, \vec{k}, z) = \frac{4\pi d}{K_0 - |2k_0 + 4\pi d F(\vec{k}, z)|}, \quad (\text{B5})$$

$$F(\vec{k}, z) = \sum_{m \neq 0; |\vec{G}_m| \leq \pi k_0} \frac{1}{z - |\vec{k} - \vec{G}_m|^2}.$$

Above the limit

$$f(\vec{k}, z) = \lim_{k_0 \rightarrow \infty} [2k_0 + 4\pi d F(\vec{k}, z)] \quad (\text{B6})$$

is finite. In reduced units (see Appendix A) and with $\delta = 4\pi d/K_0^3$ for the reduced density of atoms, the MD may be written as

according to Eq. (5) is

$$N(\vec{p}) = 8\pi K_0 / (K_0^2 + p^2)^2. \quad (\text{A5})$$

In reduced units $\epsilon = E/K_0^2$, $\vec{p} = p/K_0$, $\vec{N} = K_0^3 N$, and $\vec{J} = K_0 J$. Equation (A5) may be written as

$$\vec{N}(\vec{p}) = 8\pi / (1 + \vec{p}^2)^2. \quad (\text{A6})$$

From Eq. (10) it follows for the CP

$$\vec{J}(\vec{q}) = (1/\pi^2) [1/(1 + \vec{q}^2)] \quad (\text{A7})$$

normalized as

$$\int_{-\infty}^{\infty} \vec{J}(\vec{q}) d\vec{q} = 1. \quad (\text{A8})$$

APPENDIX B: CRYSTALLINE ARRAY OF ATOMS

For an arbitrary crystal lattice $\{\vec{R}_j\}$ with one atom per unit cell the crystal potential is given by (N atoms in volume Ω)

$$V(\vec{k}, \vec{k}') = \sum_j e^{-i(\vec{k}-\vec{k}') \cdot \vec{R}_j} v(\vec{k}, \vec{k}'). \quad (\text{B1})$$

The electronic self-energy satisfies the integral equation

$$S(\vec{k}, \vec{k}', z) = V(\vec{k}, \vec{k}') + \sum_{\vec{k}'' \neq \vec{k}} V(\vec{k}, \vec{k}'') \times \frac{1}{z - \vec{k}''^2} S(\vec{k}'', \vec{k}', z). \quad (\text{B2})$$

Using the lattice relation

$$\sum_j e^{-i(\vec{k}-\vec{k}') \cdot \vec{R}_j} = N \sum_m \delta_{\vec{k}-\vec{k}', \vec{G}_m}, \quad (\text{B3})$$

where \vec{G}_m is a reciprocal-lattice vector, and Eq. (A1), one obtains

$$\vec{N}(\vec{p}) = \frac{4\pi}{\delta} \frac{1}{|1 - \delta \vec{S}/\partial \epsilon|} \Big|_{\epsilon = \epsilon(\vec{p}) < \epsilon_F} \quad (\text{B7})$$

and

$$\vec{S}(\vec{p}, \epsilon) = \delta \frac{1}{1 - f(\vec{p}, \epsilon)}. \quad (\text{B8})$$

The energy spectrum is given by the roots of

$$\epsilon - \vec{p}^2 - \vec{S}(\vec{p}, \epsilon) = 0. \quad (\text{B9})$$

$\vec{N}(\vec{p})$ is normalized according to

$$\frac{1}{(2\pi)^3} \int d^3\vec{p} \vec{N}(\vec{p}) = 1. \quad (\text{B10})$$

APPENDIX C: RANDOM ARRAY OF ATOMS

In the CPA approximation, the self-energy for a structurally disordered system is given by the non-linear integral equation¹⁶

$$S(\vec{k}, \vec{k}', z) = dv(\vec{k}, \vec{k}') + d \sum_{\vec{k}'' \neq \vec{k}} v(\vec{k}, \vec{k}'') \frac{a_2(\vec{k}'' - \vec{k}')}{z - k''^2 - S(\vec{k}'', \vec{k}', z)} S(\vec{k}'', \vec{k}', z). \quad (C1)$$

Using the model potential (A1) and $a_2(\vec{q}) = 1$ (random distribution), one obtains

$$S(\vec{k}, \vec{k}', z) = - \left(\frac{4\pi d}{v_0} \right) \left[1 + \sum_{\vec{k}'' \neq \vec{k}, |\vec{k} - \vec{k}''| \leq \pi k_0} \frac{1}{z - k''^2 - S(\vec{k}'', \vec{k}', z)} S(\vec{k}'', \vec{k}', z) \right]. \quad (C2)$$

As in Appendix A $S(\vec{k}, \vec{k}', z) = S(z)$ for $k_0 \rightarrow \infty$. For a real energy

$$S(E) = \frac{4\pi d}{K_0 + i[E - S(E)]^{1/2}}. \quad (C3)$$

In reduced units Eq. (C3) is equivalent to the cubic equation

$$\sigma^3 - \sigma^2(\epsilon + 1) + 2\sigma\delta - \sigma^2 = 0, \quad (C4)$$

where $\sigma = S/k_0^2$. Eq. (C4) defines $\sigma(\epsilon)$ and thus the

MD is

$$\tilde{N}(\tilde{\rho}) = - \frac{4}{\delta} \int_{-\infty}^{\epsilon_F} d\epsilon \operatorname{Im} \frac{1}{\epsilon - \tilde{\rho}^2 - \sigma(\epsilon)}. \quad (C5)$$

The Fermi energy is fixed by

$$\int_{-\infty}^{\epsilon_F} d\epsilon \tilde{n}(\epsilon) = 1 \quad (C6)$$

with $\tilde{n}(\epsilon) = K_0^2 n(E)$ for the DOS.

*Work supported in part by the Deutsche Forschungsgemeinschaft.

†Present address: Fachbereich Physik, Universität Essen, Gesamthochschule, Federal Republic of Germany.

‡On leave of absence from: Electron Physics Laboratory, Helsinki University of Technology, SF-02150 Espoo 15, Finland.

¹P. M. Platzmann and N. Tzoar, Phys. Rev. **139**, A410 (1965).

²P. Eisenberger and P. M. Platzman, Phys. Rev. A **2**, 415 (1970).

³R. J. Weiss, W. A. Reed, and P. Pattison, in *Compton Scattering*, edited by B. G. Williams (McGraw-Hill, New York (to be published)).

⁴J. Rath, C. S. Wang, R. A. Tawil, and J. Callaway, Phys. Rev. B **8**, 5139 (1973).

⁵W. A. Reed, P. Eisenberger, F. Martino, and K.-F. Berggren, Phys. Rev. Lett. **35**, 114 (1975); K.-F. Berggren, F. Martino, P. Eisenberger, and W. A. Reed, Phys. Rev. B **13**, 2292 (1976).

⁶D. Stroud and H. Ehrenreich, Phys. Rev. **171**, 399 (1968).

⁷W. A. Reed, P. Eisenberger, K. C. Pandey, and L. C. Snyder, Phys. Rev. B **10**, 1507 (1974).

⁸P. Krusius, J. Phys. C **10**, 1875 (1977).

⁹A. Zunger and A. J. Freeman, Phys. Rev. B **15**, 5049 (1977).

¹⁰C. A. Coulson, Proc. Cambridge Philos. Soc. **37**, 55 (1941); C. A. Coulson, and W. E. Duncanson, *ibid.* **37**, 67 (1941); and C. A. Coulson, *ibid.* **37**, 74 (1941).

¹¹B. Kramer, P. Krusius, W. Schröder, and W. Schülke, Phys. Rev. Lett. **38**, 1227 (1977).

¹²P. Lloyd, Proc. Phys. Soc. **90**, 217 (1967).

¹³K. Maschke and P. Thomas, Phys. Status Solidi **39**, 453 (1970).

¹⁴P. Soven, Phys. Rev. **156**, 809 (1967).

¹⁵P. Soven, Phys. Rev. **178**, 1136 (1969).

¹⁶See e.g., B. Kramer, in *Physics of Structurally Disordered Solids*, edited by S. S. Mitra (Plenum, New York, 1976), p. 291.

¹⁷W. A. Reed and P. Eisenberger, Phys. Rev. B **6**, 4596 (1972).

¹⁸The CPA overestimates the width of the DOS. See e.g., H. K. Peterson, L. M. Schwartz, and W. H. Butler, Phys. Rev. B **11**, 3678 (1975) and references therein.

¹⁹U. Bonse, W. Schröder, and W. Schülke, Solid State Commun. **21**, 807 (1977).